ACS chemical biology

Articles

pubs.acs.org/acschemicalbiology

New Fluorescent Substrate Enables Quantitative and High-Throughput Examination of Vesicular Monoamine Transporter 2 (VMAT2)

Gang Hu,[†] Adam Henke,[†] Richard J. Karpowicz, Jr.,[†] Mark S. Sonders,[§] Frances Farrimond,[∥] Robert Edwards,[∥] David Sulzer,*[,‡] and Dalibor Sames*[,†]

[†]Department of Chemistry, Columbia University, New York, New York 10027, United States

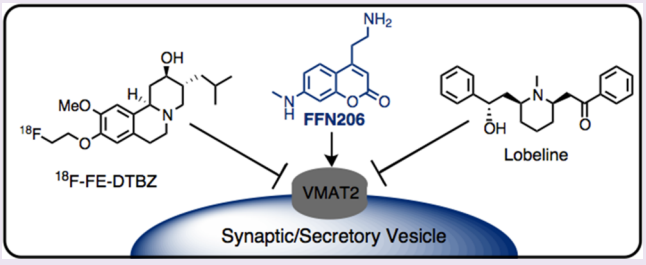
[‡]Departments of Neurology, Psychiatry, and Pharmacology, Columbia University, New York, New York 10032, United States

[§]Departments of Psychiatry and Neurology, Columbia University, New York, New York 10032, United States

[∥]Departments of Neurology and Physiology, University of California School of Medicine, San Francisco, San Francisco, California 94143, United States

Supporting Information

ABSTRACT: Vesicular monoamine transporter 2 (VMAT2) is an essential component of the monoaminergic neurotransmission system in the brain as it transports monoamine neurotransmitters from the neuronal cytosol into the synaptic vesicles and thus contributes to modulation of neurotransmitter release. Considering the continuing interest in VMAT2 as a drug target, as well as a target for the design of imaging probes, we have developed a fluorescent substrate well suited for the study of VMAT2 in cell culture. Herein, we report the synthesis and characterization of a new fluorescent probe, FFN206, as an excellent VMAT2 substrate capable of detecting VMAT2 activity in intact cells using fluorescence microscopy, with subcellular localization to VMAT2-expressing acidic compartments without apparent labeling of other organelles. VMAT2 activity can also be measured via microplate reader. The apparent K_m of FFN206 at VMAT2 was found to be 1.16 ± 0.10 μM, similar to that of dopamine. We further report the development and validation of a cell-based fluorescence assay amenable to high-throughput screening (HTS) using VMAT2-transfected HEK cells (Z′-factor of 0.7−0.8), enabling rapid identification of VMAT2 inhibitors and measurement of their inhibition constants over a broad range of affinities. FFN206 thus represents a new tool for optical examination of VMAT2 function in cell culture.



In the central nervous system (CNS), monoamine neurotransmitters (dopamine, norepinephrine, serotonin, and histamine) play important roles in modulating the strength of both excitatory (glutamate) and inhibitory (GABA) synapses via activation of the corresponding receptors.[1−3] As such, monoamines contribute to modulation of neural circuits involved in many aspects of nervous system physiology and disease.[4] Monoamines are synthesized and released by the corresponding monoamine neurons (*e.g.*, dopamine by dopamine neurons, serotonin by serotonin neurons), which provide synaptic inputs to diverse areas throughout the brain. Vesicular monoamine transporter 2 (VMAT2) is an essential component of the monoaminergic neurotransmission system in the brain as it transports monoamine neurotransmitters from the neuronal cytosol into the synaptic vesicle lumen using the proton gradient maintained by the vacuolar H^+-ATPase (Figure 1).[5−7] Consequently, inhibition of VMAT2 reduces the vesicular monoamine levels and thus the amount available for secretion. In addition to the central nervous system, VMAT2 is also found in peripheral tissues such as sympathetic ganglia and pancreatic beta cells.[5] It has been suggested that monoamine neurotransmitters are co-released with insulin and may form a regulatory feedback loop for insulin release.[8] The closely related but pharmacologically distinct isoform VMAT1 is predominantly expressed in the neuroendocrine cells such as chromaffin granule cells of the adrenal medulla.[5,9−11] Reserpine, the classical inhibitor of both VMAT1 and VMAT2, has been used as an antipsychotic and antihypertensive agent (Figure 2). *In vivo* and *in vitro* studies showed that reserpine depletes monoamine content in both CNS and peripheral tissues.[12] Although reserpine's clinical use was discontinued several decades ago due to side effects, an interest in VMAT2 as a medicinal target has been renewed in recent years.[13] For example, in 2008 the FDA approved the synthetic VMAT2 inhibitor tetrabenazine (TBZ) for treatment of chorea associated with Huntington's disease.[14] Development and

Received: April 15, 2013
Accepted: June 9, 2013

 © XXXX American Chemical Society dx.doi.org/10.1021/cb400259n | *ACS Chem. Biol.* XXXX, XXX, XXX−XXX

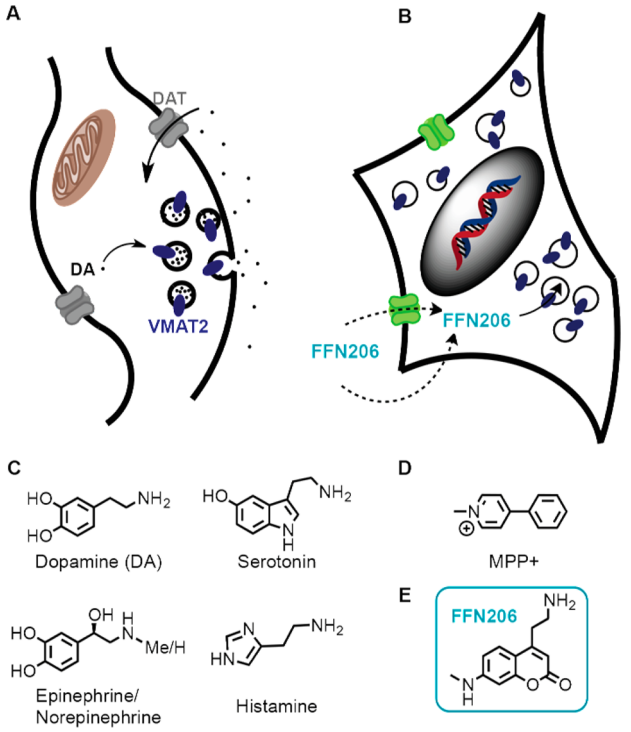


Figure 1. VMAT2 is an important component of monoamine secretory systems in the brain and periphery. (A) Schematic representation of a dopaminergic presynaptic release site as a specific example of monoaminergic presynaptic elements. Dopamine is concentrated into synaptic vesicles *via* VMAT2, a transport driven by the pH gradient between the synaptic vesicle lumen and the cytoplasm. Dopamine is released *via* exocytosis and recycled *via* dopamine transporter (DAT) on the cell surface. VMAT2 is shared by the central monoaminergic synapses. (B) Schematic representation of a VMAT2 (blue) expressing cell (VMAT2-HEK cells or pancreatic beta cells). (C) Examples of endogenous monoamine VMAT2 substrates. (D) MPP+, an example of an exogenous VMAT2 substrate. (E) Compound FFN206 is a fluorescent VMAT2 substrate developed in this work, which enables functional examination of VMAT2 in cell culture.

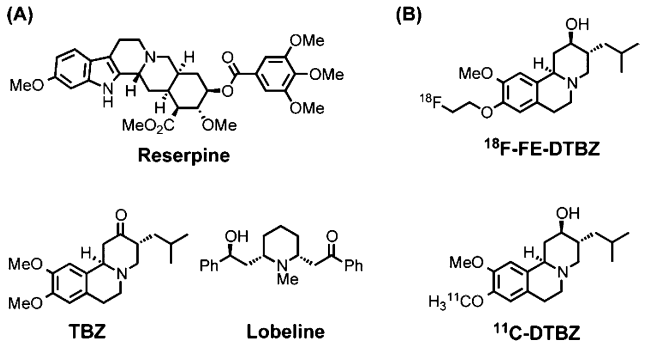


Figure 2. Chemical structures of selected examples of VMAT2 inhibitors. (A) Representative inhibitors reserpine, TBZ, and lobeline. (B) Radiolabeled TBZ derivatives for PET imaging.

examination of other VMAT2 inhibitors is actively pursued in the context of hyperkinetic movement disorders.[15]

VMAT2 inhibitors are also of interest for treatment of psychostimulant abuse and addiction. The natural product lobeline and its derivatives inhibit methamphetamine-induced dopamine release as well as methamphetamine self-administration *via* the inhibition of VMAT2. These compounds, structurally distinct from reserpine and TBZ (Figure 2), are pursued as novel therapeutics in preclinical and clinical studies of methamphetamine abuse disorders.[16,17] Further, high-affinity VMAT2 inhibitors represent a starting point for the development of diagnostic and imaging agents. A number of PET (Positron Emission Tomography) tracers targeting VMAT2 have been reported and examined as diagnostic tools in the context of neurological and psychiatric disorders.[18−21] Furthermore, VMAT2 PET probes enable imaging of beta cell mass in the pancreas and thus may provide a diagnostic agent for monitoring progression of diabetes as well as efficacy of antidiabetic treatments.[22,23]

In contrast to inhibition, upregulation of VMAT2 expression and function shows neuroprotective effects, presumably by decreasing the cytosolic catecholamines, and represents a promising experimental approach to treatment of Parkinson's disease and other neurodegenerative disorders.[13,24]

There is therefore a strong rationale for the development of new approaches and assays for measuring VMAT2 function and inhibition. Examination of VMAT2 (as well as other neurotransmitter transporters) has long relied on uptake/binding assays that use radiolabeled endogenous substrates such as [^{3}H]DA and [^{3}H]5HT or radiolabeled inhibitors like [^{3}H]-DTBZ.[25] On the other hand, the development of fluorescent transporter assays avoids the use of radioactive reagents, enables VMAT2 monitoring in intact cells and tissues, and provides subcellular spatial resolution.

The concept of a fluorescent substrate for neurotransmitter transporters has been demonstrated with ASP+, and later APP+, which are fluorescent analogs of MPP+ and substrates of plasma membrane transporters DAT, NET and SERT.[26−28] These compounds enable optical monitoring of monoamine transporter function and high-throughput screening of inhibitors.[29,30] The commercial kit for plasma membrane transporters, NTUA, using a proprietary fluorescent probe,[31] has recently been applied to the development of a fluorescence assay for VMAT2 in a transfected cell line. However, the substrate in the commercial kit labels mitochondria and other cellular organelles, creating high VMAT2-independent labeling and therefore requires separation of the VMAT2-dependent and -independent signals by fluorescence microscopy.[32]

In recent years, we have been developing fluorescent false neurotransmitter (FFNs) as fluorescent tracers that enable imaging of neurotransmitter release at single synapses.[33−35] As the first step in the design of FFNs for dopaminergic synapses, we have been developing fluorescent substrates for VMAT2, to enable loading of the synaptic vesicles with the fluorescent probe along with the native neurotransmitters. The previously developed FFNs, however, have not been useful for cultured cells and HTS format.

Here we report a new probe, FFN206, optimized for the use in an intact VMAT2-transfected cell line system and for the high-throughput assay of VMAT2 function. FFN206 is highly fluorescent, its emission is pH independent, and it is taken up by VMAT2-transfected HEK cells with a high signal-to-background ratio. Using FFN206, quantitative characterization of VMAT2 inhibitors can be accomplished using a straightforward and rapid fluorometric live cell assay. We also report on the development of a fluorometric HTS assay and demonstrate its utility with a representative compound collection spanning a wide range of VMAT2 inhibitory potency.

dx.doi.org/10.1021/cb400259n | *ACS Chem. Biol.* XXXX, XXX, XXX−XXX

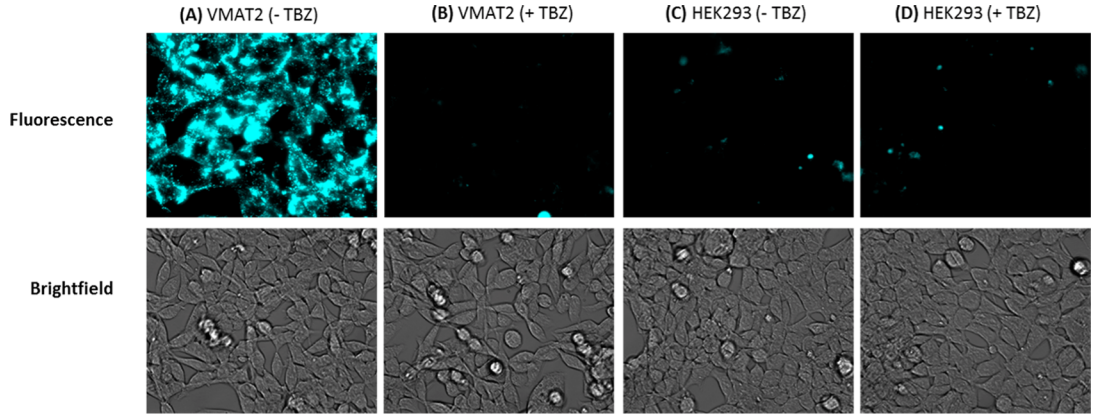


Figure 3. Uptake of FFN206 in cultured cells is dependent on VMAT2 activity: Epifluorescence images of HEK cells (VMAT2-transfected and null-transfected controls) treated with FFN206 (5 μM, 2 h incubation) in the absence or presence of TBZ (2 μM, 1 h preincubation followed by coincubation with the probe). (A) FFN206 selectively accumulates in cells expressing VMAT2. (B) Negligible uptake of FFN206 in VMAT2-HEK cells pretreated with TBZ. (C) HEK293 cells (not expressing VMAT2) pretreated with DMSO vehicle. (D) Control HEK293 cells pretreated with TBZ also accumulate negligible amounts of FFN206. Top row = epifluorescence images, bottom row = brightfield images.

RESULTS AND DISCUSSION

Design, Synthesis, and Photophysical Properties of FFN206. VMAT2 exhibits considerable plasticity in its substrate scope: it transports not only different endogenous monoamine neurotransmitters such as dopamine, norepinephrine, serotonin, and histamine (Figure 1C) but also exogenous synthetic compounds such as the neurotoxin MPP^+ (Figure 1D).[6,36,37] *In vitro* experimental data suggests that a variety of psychostimulants including amphetamine and 3,4-methylenedioxymethamphetamine (MDMA) are substrates.[25] We exploit the permissiveness of VMAT2 in amine transport to design fluorescent substrates as potential FFN candidates and in the present case as reporters of VMAT2 function.[33−35] As there is little detailed structural information about substrate-VMAT2 interactions,[5,38] we based our strategy on combining the key structural feature of monoamine substrates (the arylethylamine fragment) and the fluorescent and photostable 7-aminocoumarin system. We introduce a new probe, FFN206, (Figure 1E) as a fluorescent VMAT2 substrate optimized for use in a heterologous cell culture system.

Synthesis of FFN206 was accomplished according to a short synthetic sequence with the key step relying on the catalytic hydroarylation of alkynoate esters developed in our group (Supplementary Scheme S1).[39−41] In potassium phosphate buffer (0.1 M, pH 7.4), FFN206 absorbs light at $\lambda_{abs,max}$ = 368 nm and exhibits high fluorescence with a sizable Stokes shift: quantum yield = 0.74, extinction coefficient = 15,000 M^{-1} cm^{-1}, $\lambda_{Ex,max}$ = 369 nm, $\lambda_{Em,max}$ = 464. It was found that FFN206 is photostable to repeated measurements in a plate reader (Supplementary Figure S1). We chose to pursue studies of FFN206 as a potential fluorescent VMAT2 substrate while working toward a high-throughput assay for VMAT2 function.

Examination of FFN206 Uptake in VMAT2-Transfected HEK Cells. To examine FFN206 as a potential VMAT2 substrate, we used human embryonic kidney cells (HEK293) stably transfected with rat VMAT2 (VMAT2-HEK). These cells express VMAT2 on acidic intracellular organelles, where a vacuolar-type H^+-ATPase (V-ATPase) provides the required driving force (primarily proton gradient) for substrate transport, and represent a robust cell culture experimental system.[42] FFN206 was first evaluated in VMAT2-HEK cells with wide-field fluorescence microscopy, which enabled visualization of individual cells and the intracellular distribution of the fluorescent compounds (Figures 3 and 4). The VMAT2-HEK cells incubated with FFN206 (5 μM, 2 h) displayed a punctate fluorescent pattern consistent with accumulation of the compound in acidic organelles expressing VMAT2 (Figure 3A), while only background levels of fluorescence were observed in control HEK cells (not expressing VMAT2, Figure 3C) or in either cell type pretreated with the VMAT inhibitor TBZ (2 μM) (Figure 3B,D).

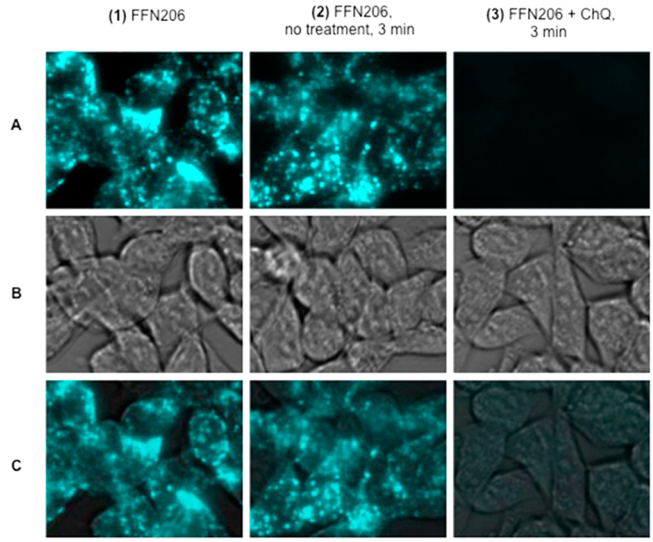


Figure 4. Uptake of FFN206 in VMAT2-HEK cells is dependent on the proton gradient. FFN206's punctate fluorescent pattern in VMAT2-HEK cells is lost following treatment with lipophilic base chloroquine. Expanded view of single cells loaded with FFN206 (5 μM), washed, and imaged. Row A: fluorescent images (λ_{ex} = 350 ± 25 nm, λ_{em} = 460 ± 25 nm). Row B: bright field images. Row C: overlay of the fluorescent and bright field images. Column (1): Cells loaded with FFN206 and imaged (5 μM). Column (2): Cells loaded with FFN206 and incubated for 3 min after washing (demonstrating the stability of signal over this time period). Column (3): Cells loaded with FFN206 and treated with chloroquine (ChQ, 100 μM) for 3 min.

To test the hypothesis that FFN206 accumulates in acidic organelles as opposed to simply binding to the protein target, we treated the cells with chloroquine, a lipophilic base that

dx.doi.org/10.1021/cb400259n | ACS Chem. Biol. XXXX, XXX, XXX−XXX

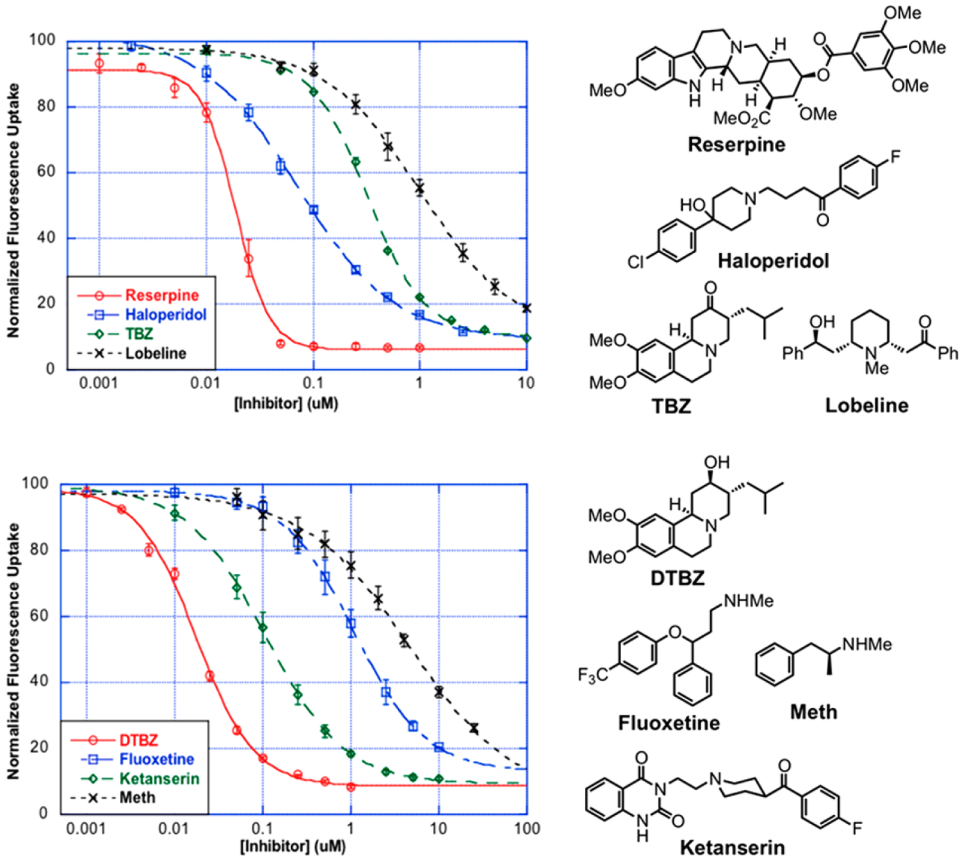


Figure 5. IC_{50} values of known VMAT2 inhibitors were measured in the FFN206 uptake assay. The final concentration for FFN206 is 1 μM. Error bars are standard errors (SE) derived from 4 independent experiments. Each experiment was run in triplicate/plate and 2 plates total. IC_{50} values are listed as [inhibitor] ± SE. Reserpine: IC_{50} = 0.019 ± 0.001 μM. Haloperidol: IC_{50} = 0.071 ± 0.003 μM. TBZ: IC_{50} = 0.32 ± 0.01 μM. Lobeline: IC_{50} = 1.01 ± 0.07 μM. DTBZ: IC_{50} = 0.017 ± 0.001 μM. Fluoxetine: IC_{50} = 1.07 ± 0.05 μM. Ketanserin: IC_{50} = 0.105 ± 0.005 μM. *S*(+)-Methamphetamine (Meth): IC_{50} = 4.53 ± 1.42 μM.

crosses membranes and collapses the proton gradient between the lumen of acidic compartments and cytosol (the "weak base effect").[43] We again observed a punctate fluorescence signal (Figure 4, row A) that was completely abolished within 3 min of treatment with chloroquine, although stable under control conditions over the same time (Figure 4, rows B,C). These results indicate that FFN206 is a VMAT2 substrate, as its uptake by HEK cells is (1) dependent on VMAT2 expression, (2) blocked by moderate concentrations of TBZ, a VMAT2-specific inhibitor, and (3) dependent on the proton gradient that drives substrate-proton antiport by VMAT2. The observation that FFN206 does not considerably label other organelles renders this compound a useful imaging agent for subcellular localization of VMAT2 activity.

Validation of the Utility of FFN206 in a Microplate Assay for VMAT2 Activity. In order to move toward a microplate-based assay for VMAT2 activity, a fluorometric assay was established to quantitatively measure VMAT2-dependent uptake in living cells, with null-transfected HEK cells used as the control. The VMAT2 inhibitor TBZ was also used as a pharmacological tool to block VMAT2 transport. The cells were grown in 96-well plates, incubated with the test compounds in the absence or presence of TBZ, washed, and the fluorescence was measured in each well by a plate reader. Monitoring the fluorescence of FFN206 (1 μM) in cells over time demonstrated that the fluorescence uptake reached a plateau in VMAT2 transfected cells at ~40 min, affording approximately a 7-fold increase in VMAT2-HEK cell fluorescence over control or inhibited cells (Supplementary Figure S2A). As a negative control we used cocaine (a DAT inhibitor that does not inhibit VMAT2), which showed no detectable inhibition of FFN206 uptake in this assay (Supplementary Figure S2B). These data are consistent with the results obtained by microscopy imaging and further support the conclusion that FFN206 is a VMAT2 substrate.

Apparent K_m of FFN206 at VMAT2. To provide a quantitative measure of FFN206's interaction with VMAT2, we next measured cellular uptake kinetics using fluorometry. The initial fluorescence uptake velocity of FFN206 in VMAT2-HEK cells remains linear for 12 min for concentrations up to 6 μM, and the initial rates were measured in the linear interval at various FFN206 concentrations. Fitting the plot to the Michaelis–Menten equation provided the apparent K_m value of 1.16 ± 0.10 μM (Supplementary Figure S3). A similar K_m was measured when cells were permeabilized with digitonin (Supplementary Figure S4), suggesting that diffusion across the plasma membrane or transport through a plasma membrane transporter is not the rate-determining step of uptake in the whole cell assay (where the vast majority of VMAT2 protein is intracellular). To confirm the apparent K_m obtained by the fluorescence assay with intact cells, the affinity of FFN206 for VMAT2 was measured by the inhibition of [^{3}H]serotonin uptake in membrane preparations obtained from VMAT2-HEK cells. An IC_{50} value of 1.15 μM was obtained (Supplementary

dx.doi.org/10.1021/cb400259n | *ACS Chem. Biol.* XXXX, XXX, XXX–XXX

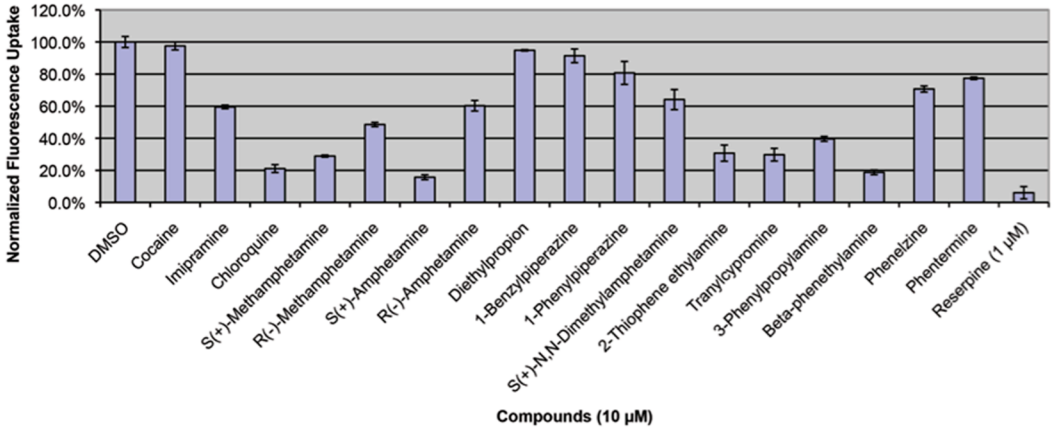


Figure 6. A selected collection of drugs was screened for VMAT2 inhibition in FFN206 uptake assay. The broad range of inhibition effects can be measured in HTS format. The cells were first incubated with 180 μL of experimental medium and 10 μL of inhibitor (20× the final concentration) for 30 min, followed by addition of 10 μL of FFN206 (20 μM) and incubation for 60 min. The final concentrations of tested compounds were 10 μM with the exception of reserpine, for which 1 μM was used. The final concentration for FFN206 was 1 μM. The uptake was terminated with one PBS buffer wash. Error bars are standard errors (SE) derived from 4 independent experiments. Each experiment was run in triplicate per plate and 2 plates total.

Figure S5), showing good agreement with the apparent K_m for FFN206 determined by fluorescence. The moderate affinity of FFN206 for VMAT2 compares well with endogenous substrates such as dopamine (K_m = 0.82−0.95 μM[6,37] and IC_{50} = 0.92 ± 0.05 μM[6]).

Quantitative Fluorometric Assay for VMAT2 Activity. This assay was created with potential high-throughput screening applications in mind. Accordingly, the assay workflow was optimized to accommodate the potential for automated screening. Namely, the required components were added in the following sequence: 180 μL of experimental medium, 10 μL (20× the final concentration) of inhibitor stock solution, and 10 μL (20 μM) of FFN206 stock solution to each well of 96-well plate containing cultured VMAT2-HEK cells. The uptake of FFN206 was terminated by one wash with PBS and then measured in PBS on a plate reader.

The established VMAT2 inhibitors reserpine, TBZ, DTBZ, lobeline, fluoxetine, *S*(+)-methamphetamine, ketanserin, and haloperidol were chosen for validation of the quantitative assay across a range of potencies (IC_{50}'s, Figure 5). Haloperidol is a potent VMAT2 inhibitor in addition to its well-recognized property as a high affinity ligand for the D2 receptor.[44] Likewise, while ketanserin is known to bind strongly to 5HT receptors,[45] it also acts as a potent inhibitor of VMAT2.[46] Each of these compounds was found to inhibit the uptake of FFN206 in a dose-responsive manner. Substitution of the apparent K_m value of FFN206 (determined above) into the Cheng−Prusoff equation ($K_i = IC_{50}(1+[S]/K_m)$) allows for the ready calculation of K_i values from the determined IC_{50}'s, assuming competitive interactions (Supplementary Table S1).

The IC_{50} and K_i values obtained by the present assay are in excellent agreement with those reported in literature (Supplementary Table S1). The standard errors of the fluorescence measurements as well as those of the calculated IC_{50} values reported herein are generally superior to those obtained in radioactive assays, indicating higher reproducibility of the optical assay. Thus, FFN206 and a standard fluorescence plate reader enables rapid determination of quantitative inhibition parameters of VMAT2 inhibitors in intact cells.

Validation of the Assay for HTS Applications. High-throughput assays are evaluated for robustness by determining the dynamic range of the assay and experimental variability (determined as standard deviations of control data sets), and HT assays are held to high standards to minimize occurrences of false positives or negatives arising from statistical variations of the normal distributions of the data. The Z'-factor has been introduced as an important means of quantifying this robustness; a Z'-factor greater than 0.5 indicates an assay is acceptable for HT screening.[47] In order to determine the applicability of the FFN206-based VMAT2 assay to high-throughput applications, control experiments were conducted from which this parameter was calculated (Z'-factor = 0.68 ± 0.07; mean ± SD, calculated from the arithmetic means determined from 5 independent experiments, each consisting of 2 identical plates; see Supplementary Figure S6). Additionally, it was found that by measuring area scans of each well (versus the single-point scans), this parameter can be further improved significantly (Supplementary Table S2), although area scans considerably slow the reading, making it less attractive for HT applications.

The fluorometric assay utilizing FFN206 is well suited for HTS as indicated by the statistical evaluation of its performance ($Z' > 0.5$ is recommended for HTS). It should be noted that automation of the assay, from cell counting to automated washing and solution delivery, would likely improve this parameter even further.

Experimental Screen of a Small Compound Collection. In order to demonstrate utility of the assay in practice, a collection of plasma membrane transporter inhibitors and substrates were screened at a concentration of 10 μM, which is a commonly used concentration for initial screens of compound collections. The inhibitory effect on VMAT2 was determined by measuring FFN206 uptake, as above. DMSO (0.1% v/v) and reserpine (1 μM) were used in this assay as controls (Figure 6). The basic parameters regarding the quality of the assay in practical use were thus assessed on the basis of 4 independent experiments. The experimental Z'-factor was determined from the assay controls of each plate (DMSO and reserpine) to be Z' = 0.76 ± 0.07 (mean ± SD), indicating a robust assay in practice, well above the requisite minimum Z'-value of 0.5.

As can be seen in Figure 6, this compound set afforded a wide spread of inhibitory effects (*i.e.*, percentage of inhibition),

dx.doi.org/10.1021/cb400259n | *ACS Chem. Biol.* XXXX, XXX, XXX−XXX

demonstrating the range and utility of the assay. For example, the assay showed a large difference (>40%) between the enantiomers *S*(+)-amphetamine and *R*(−)-amphetamine in their ability to inhibit FFN206 uptake (Figure 6), which is consistent with reported IC_{50} values of 3.27 and 29.0 μM, respectively (IC_{50}'s were determined by inhibiting [^{3}H]DA uptake into rat brain vesicles).[25] Similarly, the inhibition effect differed by ∼20% between *S*(+)-methamphetamine and *R*(−)-methamphetamine, also consistent with reported IC_{50} values of 9.10 μM and 19.3 μM, respectively.[25] Comparison among the *S*(+)-amphetamines with a different degree of *N*-methylation shows that inhibitory effects decrease with increasing *N*-methylation. Additionally, cocaine, diethylpropion, benzylpiperazine, and phentermine have been reported to be inactive in inhibiting vesicular uptake of [^{3}H]DA by VMAT.[25] Consistently, our assay revealed no or weak inhibitory effects of these compounds on VMAT2 transport. Importantly, these results were highly reproducible from experiment to experiment, as evidenced by the small standard errors (Figure 6).

Chloroquine was included in the test to highlight potential false positives, in this case a lipophilic weak base that reduces VMAT2-dependent uptake by collapsing the pH gradient of acidic organelles (weak base effect)[43] and not through inhibition of the transporter (Figure 6, see also Figure 4). Similarly, inhibitors of v-ATPase would also afford false positive hits. As is the case for all HTS campaigns, secondary assays are needed to filter the false positives. In this case, we suggest the same format secondary assay using a LysoTracker probe or acridine orange, amphiphilic weak base dyes that accumulate in acidic organelles independently of transporters, to measure alkalinization of acidic compartments within the cell. Additional secondary assays would need to address potential fluorescence quenching of FFN206 and the possibility that a hit compound blocks a putative plasma membrane transporter that might be involved in FFN206 uptake. The digitonin-induced permeabilization of cells used in this work may serve well as a secondary assay for the latter case.

Using the same VMAT2-HEK cell line, Mini202/FFN202 has recently been reported as a pH-sensitive VMAT2 substrate.[34] This probe is not well suited for HTS, however, as the pH sensitivity may complicate VMAT2 uptake measurements. Also, Mini202/FFN202 is not as bright as FFN206, yielding a smaller dynamic range. FFN511 is not well suited for cell culture applications due to a high background signal.

A fluorescent VMAT2 assay has been reported recently using the Neurotransmitter Transporter Uptake Assay Kit (NTUA, Molecular Devices).[32] This report also demonstrates that the proprietary fluorescent DAT, NET, and SERT substrate in this kit is also a VMAT substrate. While this assay is readily applicable to HTS format, it necessitates microscopy image acquisition/processing/analysis of each well due to VMAT-independent staining of mitochondria and other cellular organelles by the NTUA probe. The FFN206 assay described here addresses this issue and enables fluorometric measurement with a standard plate reader, facilitating both the high-throughput screening for new hits and quantitative examination of identified compounds. However, the VMAT2 assay using the NTUA kit may be a better choice for examination/screening of VMAT2 function in primary dopamine neuronal culture (or other monoamine neurons) as the uptake of the NTUA probe by dopamine neurons is facilitated by DAT on the plasma membrane. The latter point is likely to be important for experimental systems with lower endogenous expression of VMAT2 in comparison to systems with high heterologous VMAT2 expression.

Conclusions. We have introduced FFN206 as a new optical probe with several applications in the study of VMAT2 in cell culture. FFN206 is capable of determining subcellular location of VMAT2-expressing organelles using fluorescence microscopy. It is also capable of reporting on VMAT2 activity in a fluorometric format highly amenable to high-throughput screening; the assay is featured with simple operations amenable for automation and excellent *Z*′-factor, as well as reproducibility. As such, FFN206 represents a new probe capable of facilitating the search for next generations of VMAT2 modulators including inhibitors, substrates, or enhancers.

METHODS

Cell Growth. The HEK GNTI$^-$ (nonglycosylating) cell line stably expressing VMAT2 (VMAT2-HEK) and HEK GNTI$^-$ cell line stably transfected with TetR (HEK) to serve as a control have been previously described.[42] Cells were grown in complete growth medium (DMEM + GlutaMAX (Life Technologies) with 10% (v/v) fetal bovine serum (FBS) (Atlanta Biologicals), 100 U/mL penicillin (Life Technologies), and 100 μg/mL streptomycin (Life Technologies)). On the day of experiments, the growth medium was replaced by experimental medium (DMEM minus phenol red (Life Technologies) with 4 mM L-glutamine (Life Technologies), 1% (v/v) charcoal/dextran-treated FBS (Atlanta Biologicals), 100 U/mL penicillin (Life Technologies), and 100 μg/mL streptomycin (Life Technologies)).

Procedure for Fluorescence Microscopy Imaging of FFN206. VMAT2-HEK cells or their respective controls, HEK293, were plated onto poly-D-lysine (Sigma-Aldrich, concentration = 0.1 mg/mL)-coated clear-bottom six-well plates at a density of 0.15−0.20 × 10^6 cells per well and grown at 37 °C in 5% CO_2. Following ∼4 days of growth, the cells appeared fibroblastic and had reached 80−90% confluence. The culture medium was removed by aspiration, and the cells were washed with PBS buffer (Life Technologies, 2.0 mL/well). To investigate the VMAT2 inhibitory effects of tetrabenazine (TBZ, Sigma-Aldrich) or reserpine (Sigma-Aldrich), cells were incubated in 1.0 mL of experimental media containing the respective inhibitor (4 μM prepared from 10 mM stock solution in DMSO) or DMSO vehicle as a control at 37 °C in 5% CO_2 for 2 h. The compound uptake was initiated by adding 1.0 mL of experimental media containing FFN206 (10 μM, prepared from a 10 mM stock solution in DMSO, with a final probe concentration of 5 μM in the uptake assay). Following incubation at 37 °C in 5% CO_2 for 2 h, the media was removed by aspiration, and the cells were washed with PBS (2 mL/well) and maintained in fresh experimental media (1 mL/well). Fluorescence images (at least 3 images/well in duplicate plates) were acquired with a Leica FW 4000 imaging system (Leica Microsysytems, Wetzlar, Germany) equipped with a Chroma custom filter cube (ex = 350 ± 25 nm, em = 460 ± 25 nm; Chroma Technology Corporation, Bellows Falls, VT) and a Hamamatsu digital camera C4742-95 (Hamamatsu Photonics, Hamamatsu, Japan). Fluorescent and bright field images were acquired with exposure time set at 800 and 37 ms, respectively. All images were adjusted using the same contrast and brightness level using ImageJ software (National Institutes of Health).

Chloroquine-Induced Redistribution of FFN206. To study chloroquine-induced redistribution of FFN, VMAT2-HEK cells preloaded with FFN206 (described above) were washed once with 2 mL of PBS buffer and maintained in 1 mL of experimental media containing 100 μM chloroquine. Following incubation for 3 min, fluorescent images were acquired by the same procedure described above. In the control experiment where no drugs were added (DMSO vehicle), the retention of FFN206 accumulation can be generally maintained for at least 1 h.

Procedure for Fluorometric Assay for High-Throughput Screening and IC_{50} Measurements of VMAT2 Inhibitors. Stably

dx.doi.org/10.1021/cb400259n | *ACS Chem. Biol.* XXXX, XXX, XXX−XXX

VMAT2-transfected HEK cells were seeded at a density of 0.03−0.04 × 10^6 cells/well in white solid-bottom 96-well plates and allowed to proliferate in growth medium for ∼3 days at 37 °C in an incubator to reach confluence. At assay, the culture medium was aspirated followed by addition of 180 μL of experimental medium to each well. The test inhibitors (10 μL of a 200 μM inhibitor in experimental medium) or DMSO vehicle prediluted in experimental medium were then added. The cells were incubated for 30 min at 37 °C, and then FFN206 (10 μL/well of 20 μM solution in experimental medium) was added. The cells were incubated for 1 h at 37 °C. The final assay concentrations for inhibitors and FFN206 were 10 μM and 1 μM, respectively, with reserpine (1 μM) serving as a positive control for inhibition. The uptake of FFN206 was terminated by one PBS buffer wash (200 μL/well) followed by addition of fresh PBS buffer (120 μL/well). The fluorescence uptake in cells was immediately recorded on a MicroMax 384 plate reader connected to a Jobin Yvon Fluorolog 3 fluorometer with excitation and emission wavelengths set at 369 and 464 nm, respectively.

To determine the IC_{50} values of inhibitors, cells were treated with varying concentrations of inhibitors as indicated. The corresponding inhibition data were normalized and fitted using KaleidaGraph (Synergy Software) [equation: y = (range)/[1 + ([I]/IC_{50})^S]+ background] to give IC_{50} values. According to the Cheng−Prusoff equation (K_i = IC_{50}/(1+[S]/K_m)), the K_i parameter, which is independent of the substrate concentration in the assay, can be calculated from the IC_{50} value if one assumes a competitive interaction. The IC_{50} values measured by this protocol and K_i values (±SEM) calculated from them are listed in Supplementary Table S1 and compared with literature values.

■ ASSOCIATED CONTENT

Supporting Information

Chemical syntheses, structural and photophysical characterization of FFN206, cellular imaging protocols, fluorometric assay and kinetics protocols, and radio-substrate assay protocols. This material is available free of charge *via* the Internet at http://pubs.acs.org.

■ AUTHOR INFORMATION

Corresponding Author

*E-mail: ds43@columbia.edu; sames@chem.columbia.edu.

Notes

The authors declare no competing financial interest.

■ ACKNOWLEDGMENTS

D. Sames was supported by the G. Harold & Leila Y. Mathers Charitable Foundation and the National Institute of Mental Health (MH086545). D. Sulzer received funding from NIDA (DA07418 and DA10154), The Udall Center for Excellence in Parkinson's Disease Research, and the JPB and Parkinson's Disease Foundations. R. Edwards was supported by grants from NIMH (MH50712) and NIDA (DA10154). Enantiopure methamphetamine, amphetamine, and *N*,*N*-dimethylamphetamine used in this study were kindly provided by Kevin Gormley of the NIDA Drug Supply Program (NDSP).

■ REFERENCES

(1) Bamford, N. S., Zhang, H., Schmitz, Y., Wu, N.-P., Cepeda, C., Levine, M. S., Schmauss, C., Zakharenko, S. S., Zablow, L., and Sulzer, D. (2004) Heterosynaptic dopamine neurotransmission selects sets of corticostriatal terminals. *Neuron 42*, 653−663.

(2) Ellender, T. J., Huerta-Ocampo, I., Deisseroth, K., Capogna, M., and Bolam, J. P. (2011) Differential modulation of excitatory and inhibitory striatal synaptic transmission by histamine. *J. Neurosci. 31*, 15340−15351.

(3) Mathur, B. N., Capik, N. A., Alvarez, V. A., and Lovinger, D. M. (2011) Serotonin induces long-term depression at corticostriatal synapses. *J. Neurosci. 31*, 7402−7411.

(4) Verhoeff, N. P. (1999) Radiotracer imaging of dopaminergic transmission in neuropsychiatric disorders. *Psychopharmacology (Berlin, Ger.) 147*, 217−249.

(5) Wimalasena, K. (2011) Vesicular monoamine transporters: structure-function, pharmacology, and medicinal chemistry. *Med. Res. Rev. 31*, 483−519.

(6) Liu, Y., Peter, D., Roghani, A., Schuldiner, S., Prive, G. G., Eisenberg, D., Brecha, N., and Edwards, R. H. (1992) A cDNA that suppresses MPP+ toxicity encodes a vesicular amine transporter. *Cell 70*, 539−551.

(7) Liu, Y., Roghani, A., and Edwards, R. H. (1992) Gene transfer of a reserpine-sensitive mechanism of resistance to N-methyl-4-phenylpyridinium. *Proc. Natl. Acad. Sci. U.S.A. 89*, 9074−9078.

(8) Raffo, A., Hancock, K., Polito, T., Xie, Y., Andan, G., Witkowski, P., Hardy, M., Barba, P., Ferrara, C., Maffei, A., Freeby, M., Goland, R., Leibel, R. L., Sweet, I. R., and Harris, P. E. (2008) Role of vesicular monoamine transporter type 2 in rodent insulin secretion and glucose metabolism revealed by its specific antagonist tetrabenazine. *J. Endocrinol. 198*, 41−49.

(9) Peter, D., Liu, Y., Sternini, C., de Giorgio, R., Brecha, N., and Edwards, R. H. (1995) Differential expression of two vesicular monoamine transporters. *J. Neurosci. 15*, 6179−6188.

(10) Peter, D., Jimenez, J., Liu, Y., Kim, J., and Edwards, R. H. (1994) The chromaffin granule and synaptic vesicle amine transporters differ in substrate recognition and sensitivity to inhibitors. *J. Biol. Chem. 269*, 7231−7237.

(11) Erickson, J. D., Schafer, M. K., Bonner, T. I., Eiden, L. E., and Weihe, E. (1996) Distinct pharmacological properties and distribution in neurons and endocrine cells of two isoforms of the human vesicular monoamine transporter. *Proc. Natl. Acad. Sci. U.S.A. 93*, 5166−5171.

(12) Carlsson, A. (1966) Modification of sympathetic fuction. *Pharmacol. Rev. 18*, 541−549.

(13) Zheng, G., Dwoskin, L. P., and Crooks, P. A. (2006) Vesicular monoamine transporter 2: Role as a novel target for drug development. *AAPS J. 8*, E682−E692.

(14) Group, H. S. (2006) Tetrabenazine as antichorea therapy in Huntington disease: a randomized controlled trial. *Neurology 66*, 366−372.

(15) Kenney, C., and Jankovic, J. (2006) Tetrabenazine in the treatment of hyperkinetic movement disorders. *Expert Rev. Neurother. 6*, 7−17.

(16) Nickell, J. R., Krishnamurthy, S., Norrholm, S., Deaciuc, G., Siripurapu, K. B., Zheng, G., Crooks, P. A., and Dwoskin, L. P. (2010) Lobelane inhibits methamphetamine-evoked dopamine release via inhibition of the vesicular monoamine transporter-2. *J. Pharmacol. Exp. Ther. 332*, 612−621.

(17) Horton, D. B., Siripurapu, K. B., Zheng, G., Crooks, P. A., and Dwoskin, L. P. (2011) Novel N-1,2-dihydroxypropyl analogs of lobelane inhibit vesicular monoamine transporter-2 function and methamphetamine-evoked dopamine release. *J. Pharmacol. Exp. Ther. 339*, 286−297.

(18) Zhu, L., Liu, J., and Kung, H. F. (2009) Synthesis and evaluation of 2-amino-dihydrotetrabenzine derivatives as probes for imaging vesicular monoamine transporter-2. *Bioorg. Med. Chem. Lett. 19*, 5026−5028.

(19) Zubieta, J.-K., Taylor, S. F., Huguelet, P., Koeppe, R. A., Kilbourn, M. R., and Frey, K. A. (2001) Vesicular monoamine transporter concentrations in bipolar disorder type I, schizophrenia, and healthy subjects. *Biol. Psychiatry 49*, 110−116.

(20) Kilbourn, M. R. (1997) In vivo radiotracers for vesicular neurotransmitter transporters. *Nucl. Med. Biol. 24*, 615−619.

(21) Koeppe, R. A., Gilman, S., Joshi, A., Liu, S., Little, R., Junck, L., Heumann, M., Frey, K. A., and Albin, R. L. (2005) 11C-DTBZ and 18F-FDG PET measures in differentiating dementias. *J. Nucl. Med. 46*, 936−944.

(22) Souza, F., Simpson, N., Raffo, A., Saxena, C., Maffei, A., Hardy, M., Kilbourn, M., Goland, R., Leibel, R., Mann, J. J., Van Heertum, R., and Harris, P. E. (2006) Longitudinal noninvasive PET-based β cell mass estimates in a spontaneous diabetes rat model. *J. Clin. Invest. 116*, 1506−1513.
(23) Simpson, N. R., Souza, F., Witkowski, P., Maffei, A., Raffo, A., Herron, A., Kilbourn, M., Jurewicz, A., Herold, K., Liu, E., Hardy, M. A., Van Heertum, R., and Harris, P. E. (2006) Visualizing pancreatic β-cell mass with [11C]DTBZ. *Nucl. Med. Biol. 33*, 855−864.
(24) Guillot, T. S., Richardson, J. R., Wang, M. Z., Li, Y. J., Taylor, T. N., Ciliax, B. J., Zachrisson, O., Mercer, A., and Miller, G. W. (2008) PACAP38 increases vesicular monoamine transporter 2 (VMAT2) expression and attenuates methamphetamine toxicity. *Neuropeptides 42*, 423−434.
(25) Partilla, J. S., Dempsey, A. G., Nagpal, A. S., Blough, B. E., Baumann, M. H., and Rothman, R. B. (2006) Interaction of amphetamines and related compounds at the vesicular monoamine transporter. *J. Pharmacol. Exp. Ther. 319*, 237−246.
(26) Schwartz, J. W., Blakely, R. D., and DeFelice, L. J. (2003) Binding and transport in norepinephrine transporters. *J. Biol. Chem. 278*, 9768−9777.
(27) Blakely, R. D., Mason, J. N., Tomlinson, I. D., and Rosenthal, S. J. (2011) *Fluorescent substrates for neurotransmitter transporters*, U.S. Patent 7947255.
(28) Solis, E., Zdravkovic, I., Tomlinson, I. D., Noskov, S. Y., Rosenthal, S. J., and De Felice, L. J. (2012) 4-(4-(Dimethylamino)-phenyl)-1-methylpyridinium (APP+) is a fluorescent substrate for the human serotonin transporter. *J. Biol. Chem. 287*, 8852−8863.
(29) Fowler, A., Seifert, N., Acker, V., Woehrle, T., Kilpert, C., and de Saizieu, A. (2006) A nonradioactive high-throughput/high-content assay for measurement of the human serotonin reuptake transporter function in vitro. *J. Biomol. Screen. 11*, 1027−1034.
(30) Wagstaff, R., Hedrick, M., Fan, J., Crowe, P. D., and DiSepio, D. (2007) High-throughput screening for norepinephrine transporter inhibitors using the FLIPRTetra. *J. Biomol. Screen. 12*, 436−441.
(31) Jørgensen, S., Nielsen, E. Ø., Peters, D., and Dyhring, T. (2008) Validation of a fluorescence-based high-throughput assay for the measurement of neurotransmitter transporter uptake activity. *J. Neurosci. Methods 169*, 168−176.
(32) Bernstein, A. I., Stout, K. A., and Miller, G. W. (2012) A fluorescent-based assay for live cell, spatially resolved assessment of vesicular monoamine transporter 2-mediated neurotransmitter transport. *J. Neurosci. Methods 209*, 357−366.
(33) Gubernator, N. G., Zhang, H., Staal, R. G. W., Mosharov, E. V., Pereira, D. B., Yue, M., Balsanek, V., Vadola, P. A., Mukherjee, B., Edwards, R. H., Sulzer, D., and Sames, D. (2009) Fluorescent false neurotransmitters visualize dopamine release from individual presynaptic terminals. *Science 324*, 1441−1444.
(34) Lee, M., Gubernator, N. G., Sulzer, D., and Sames, D. (2010) Development of pH-responsive fluorescent false neurotransmitters. *J. Am. Chem. Soc. 132*, 8828−8830.
(35) Rodriguez, P. C., Pereira, D. B., Borgkvist, A., Wong, M. Y., Barnard, C., Sonders, M. S., Zhang, H., Sames, D., and Sulzer, D. (2013) Fluorescent dopamine tracer resolves individual dopaminergic synapses and their activity in the brain. *Proc. Natl. Acad. Sci. U.S.A. 110*, 870−875.
(36) Yelin, R., and Schuldiner, S. (1995) The pharmacological profile of the vesicular monoamine transporter resembles that of multidrug transporters. *FEBS Lett. 377*, 201−207.
(37) Gasnier, B., Roisin, M. P., Scherman, D., Coornaert, S., Desplanches, G., and Henry, J. P. (1986) Uptake of meta-Iodobenzylguanidine Granule Membranes by Bovine Chromaffin Granule Membranes. *Mol. Pharmacol. 29*, 275−280.
(38) Reith, M. E. A. (2002) *Neurotransmitter Transporters: Structure, Function, and Regulation*, 2nd ed., Humana Press, Totowa, NJ.
(39) Pastine, S. J., Youn, S. W., and Sames, D. (2003) Pt(IV)-catalyzed cyclization of arene−alkyne substrates via intramolecular electrophilic hydroarylation. *Org. Lett. 5*, 1055−1058.
(40) Pastine, S. J., Youn, S. W., and Sames, D. (2003) Pt(IV)-catalyzed cyclization of arene−alkyne substrates via C−H bond functionalization. *Tetrahedron 59*, 8859−8868.
(41) Vadola, P. A., and Sames, D. (2012) Catalytic coupling of arene C−H bonds and alkynes for the synthesis of coumarins: substrate scope and application to the development of neuroimaging agents. *J. Org. Chem. 77*, 7804−7814.
(42) Adam, Y., Edwards, R. H., and Schuldiner, S. (2008) Expression and function of the rat vesicular monoamine transporter 2. *Am. J. Physiol.: Cell Physiol. 294*, C1004−C1011.
(43) Sabban, E. L., Schwartz, J., and McMahon, A. (1990) Effect of compounds which disrupt proton gradients on secretion of neurosecretory proteins from pc12 pheochromocytoma cells. *Neuroscience 38*, 561−570.
(44) Yasumoto, S., Tamura, K., Karasawa, J., Hasegawa, R., Ikeda, K., Yamamoto, T., and Yamamoto, H. (2009) Inhibitory effect of selective serotonin reuptake inhibitors on the vesicular monoamine transporter 2. *Neurosci. Lett. 454*, 229−232.
(45) Leysen, J. E., Niemegeers, C. J., Van Nueten, J. M., and Laduron, P. M. (1982) [3H]Ketanserin (R 41 468), a selective 3H-ligand for serotonin2 receptor binding sites. *Mol. Pharmacol. 21*, 301−314.
(46) Darchen, F., Scherman, D., Laduron, P. M., and Henry, J.-P. (1998) Ketanserin binds to the monoamine transporter of chromaffin granules and of synaptic vesicles. *Mol. Pharmacol. 33*, 672−677.
(47) Zhang, J.-H., Chung, T. D. Y., and Oldenburg, K. R. (1999) A simple statistical parameter for use in evaluation and validation of high throughput screening assays. *J. Biomol. Screen. 4*, 67−73.